

Measurement of three-bond coupling constants in the osmoregulated periplasmic glucan of *Burkholderia solanacearum*

G. Lippens^{a,*}, J.-M. Wieruszkeski^a, P. Talaga^{b,**} and J.-P. Bohin^b

^aCNRS URA 1309, Pasteur Institute of Lille, 1, rue du Professeur Calmette, F-59019 Lille, France

^bCNRS UMR 111, Université des Sciences et Technologies de Lille,
F-59655 Villeneuve d'Ascq Cédex, France

Received 19 March 1996

Accepted 5 August 1996

Keywords: Cyclic oligosaccharides; Three-bond coupling constants; Isotopic enrichment

Summary

The cyclic osmoregulated periplasmic glucan produced by *Burkholderia solanacearum* contains 13 glucose units, all β -(1-2) linked except for one α -(1-6) linkage. We report here the measurement of the $^3J(\text{C1-H2}')$ and $^3J(\text{H1-C2}')$ coupling constants, characterizing the glycosidic linkages, through the use of a $^{13}\text{C}/^{12}\text{C}$ double half-filtered NOESY experiment. The values obtained give information about the (Φ, Ψ) angles of the different linkages. The results presented form an important step towards a detailed experimental model of the cyclic glucan, which might allow us to clarify its biological role and establish whether the cavity of these molecules is compatible with the capability of complexing host molecular signals.

Introduction

The structure of cyclic osmoregulated periplasmic glucans (OPGs), synthesized by different gram-negative bacteria, might shed light on the role that these molecules play in the adaptation to osmotic stress and in the phytopathogenicity of these bacteria (Breedveld and Miller, 1994). The cyclic nature of these molecules could be essential for these two aspects, but a precise structural model is needed to assess this point. The glucans produced by members of the *Rhizobiaceae* family are cyclic molecules composed of 17 to 40 glucose units, all β -(1-2) linked; their structure determination presents an enormous challenge, as the NMR spectrum of a purified subspecies is completely degenerate and equivalent to that of a single D-glucopyranosyl unit (Poppe et al., 1993; Serrano et al., 1993; André et al., 1995a,b). Recently, the structures of two fundamentally different cyclic glucans extracted from cells of *Xanthomonas campestris* (Lippens et al., 1995; York, 1995; Talaga et al., 1996) and *Burkholderia solanacearum* (Lippens et al., 1995; Talaga et al., 1996) have been described. Although they share the cyclic nature with the OPGs of members of the *Rhizobiaceae*

family, they can be distinguished by their unique degree of polymerization (DP; 16 units or 13 units) and one α -(1-6) linkage, whereas all other glucose residues are connected by β -(1-2) linkages. The presence of this α -(1-6) linkage induces structural constraints in this molecule to such an extent that all individual anomeric proton resonances can be distinguished (Fig. 1). Its minimal size and the complete resonance assignment of the cyclic OPG from *B. solanacearum* make this molecule an ideal candidate for a detailed structural study.

The scarceness of experimental constraints in oligosaccharides makes an accurate structure determination extremely challenging. In proteins, sequential assignment can be obtained from NOE contacts between neighbouring residues or on the basis of J-coupling in triple-resonance experiments (Ikura et al., 1990; Bax and Ikura, 1991; Kay et al., 1991), but the 3D structure is calculated on the basis of a large number of long-range NOE constraints. For the cyclic glucan under study, the experimental parameters used for the sequential assignment are the only ones available for the complete structure determination. We recently measured with high accuracy the interglycosidic distances H1-H2' through the use of the off-resonance ROESY tech-

*To whom correspondence should be addressed.

**Present address: Complex Carbohydrate Research Center, The University of Georgia, 220 Riverbend Road, Athens, GA 30602-4712, U.S.A.

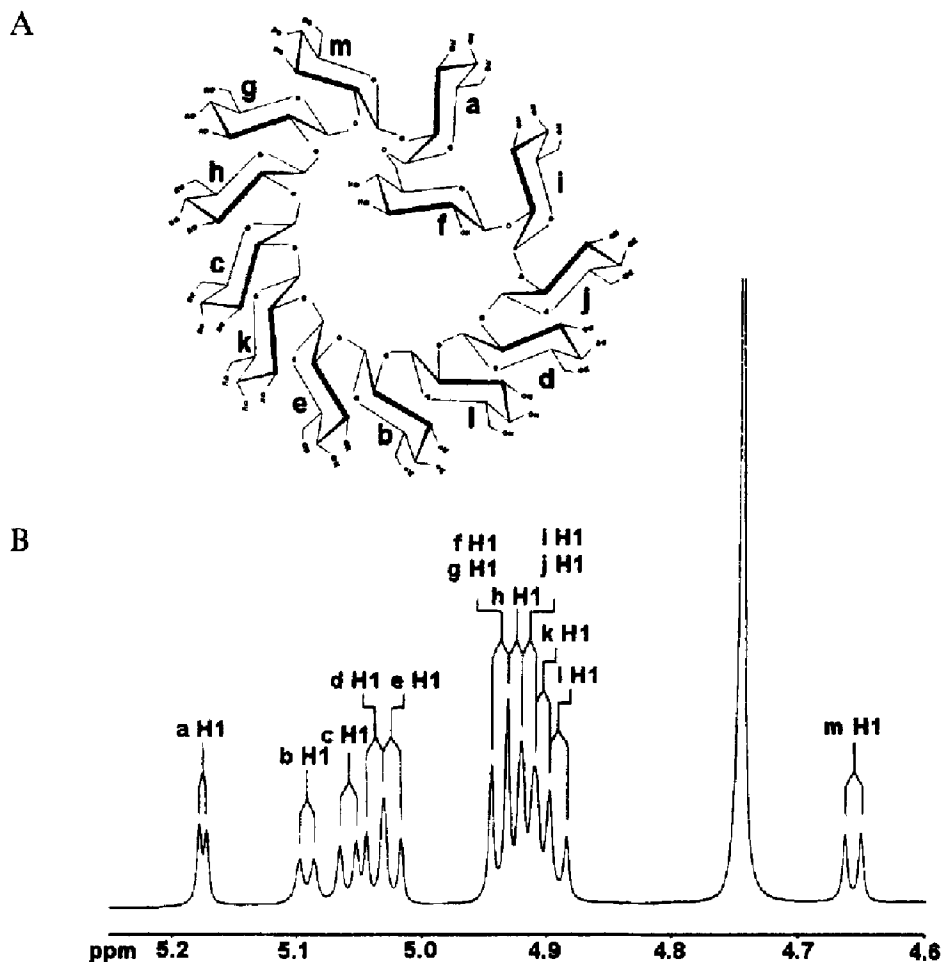


Fig. 1. Primary structure (A) and the anomeric proton spectrum (B) of the cyclic OPG of *Burkholderia solanacearum*.

nique (Lippens et al., 1996). Here, we report the determination of the 3J interglycosidic coupling constants, which, in conjunction with a Karplus relationship (Tvaroska et al., 1989), can be used to obtain information about the dihedral angles of the different glycosidic linkages.

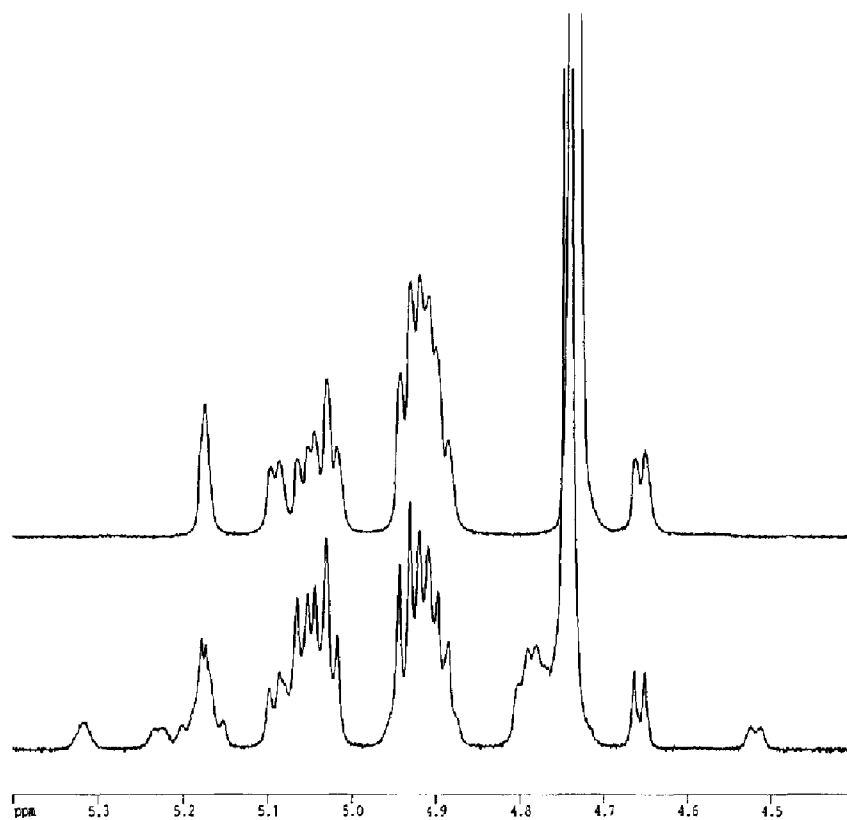
Materials and Methods

B. solanacearum T11 was grown at 24 °C by agitation in a low osmolarity medium containing K_2HPO_4 (1 mM), $(NH_4)_2SO_4$ (1.5 mM), $MgCl_2$ (0.08 mM), $FeSO_4$ (0.5 mg l^{-1}), thiamine (2 mg l^{-1}), and casein hydrolysate (4 g l^{-1} ; casamino acids, vitamin free, Difco Laboratories, Detroit, MI, U.S.A.). This medium was adjusted to pH 7.0 with Tris-free base. ^{13}C enrichment was obtained by replacing one fourth of the casein hydrolysate by an equal amount of a mixture of uniformly enriched amino acids and glucose ('sugar mix', EMBL, Heidelberg, Germany). The cyclic glucan was purified from cell extract as described previously (Talaga et al., 1996). All samples were prepared by dissolving the glucan in 500 μl D_2O . Final NMR sample concentrations were 24 mM for the natural abundance sample and 5 mM for the ^{13}C -enriched sample.

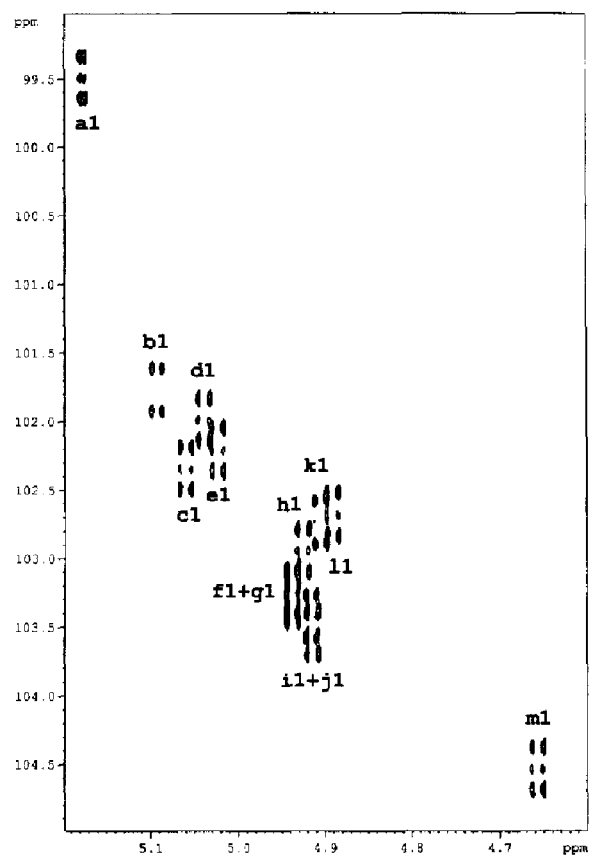
Matrix-assisted laser-desorption time of flight spectrometry (MALD-TOF) was performed as described previously (York, 1995).

NMR experiments were performed at 301 K on a Bruker DMX-600 spectrometer equipped with a triple-resonance probehead with a self-shielded z-gradient. The HMBC spectra (Bax and Summers, 1986) on the non-enriched sample included a low-pass J-filter to suppress one-bond correlations. The delay for the establishment of the long-range correlations was set to 100 ms. The double half-filtered NOESY spectrum was acquired using the States-TPPI method for quadrature detection in t_1 (Marion et al., 1989). The delays were set to $\delta = 1/4J = 1.52$ ms and $\Delta = 1/2J = 3.04$ ms, assuming an average one-bond coupling constant of 165 Hz. The final data matrix contained 256 (t_1) * 2048 (t_2) complex points, for a spectral width of 1.502 kHz. With a combined relaxation and acquisition delay of 1.3 s and 416 scans per increment, the total experiment took 87 h. After multiplication with a shifted Gaussian in both dimensions, the final matrix was transformed with 16K points in the ω_2 direction, giving a digital resolution of 0.1 Hz/point in this dimension.

A



B



C

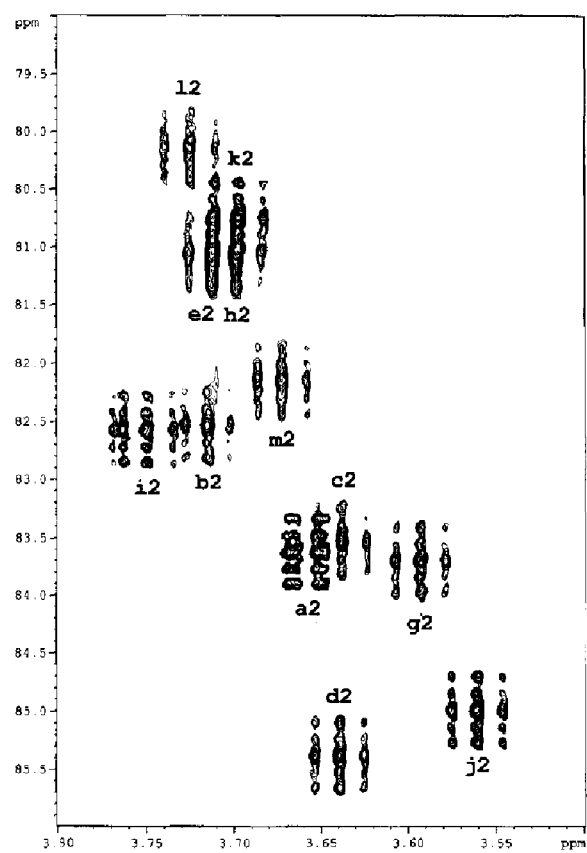


Fig. 2. (A) 1D spectrum of the ^{13}C -enriched sample of the cyclic OPG with (upper) and without (lower) ^{13}C decoupling. (B) H1-C1 region of a regular HSQC spectrum, where the ^{13}C - ^{13}C couplings have not been refocused during t_1 . (C) H2-C2 region of the same spectrum, showing the quintuplets in the ω_1 direction.

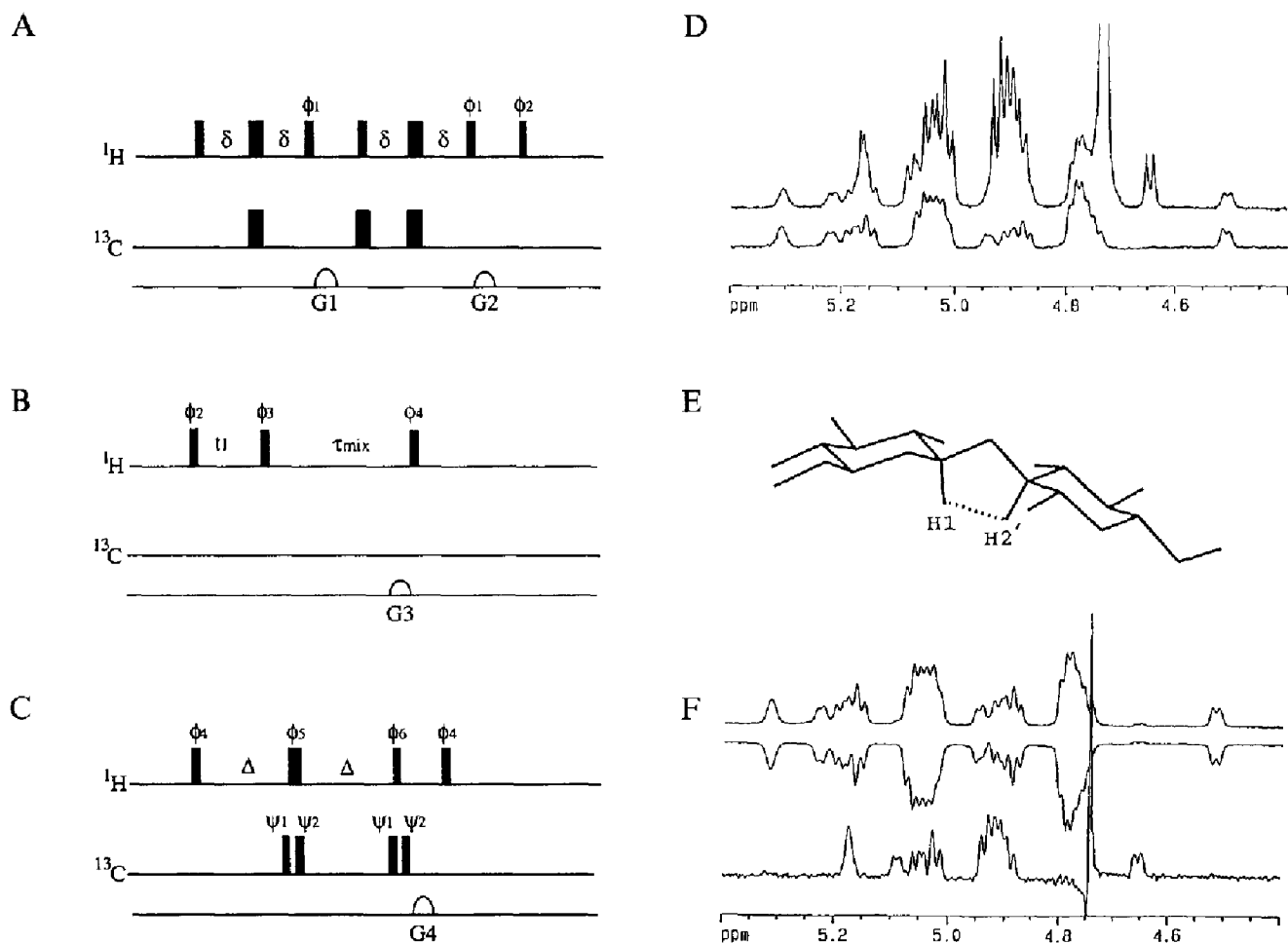


Fig. 3. Pulse sequence for the double half-filtered NOESY spectrum. The sequence has been divided into three parts, the ^{13}C filter (A) and the resulting ^{13}C -filtered 1D ^1H spectrum (D, lower trace) compared to the non-decoupled proton spectrum (D, upper trace), the t_1 evolution and subsequent NOE mixing time (B) during which the NOE transfer between the H1-H2' protons will take place (E), and the final ^{13}C filter (C) and the resulting ^1H spectrum (F, lower trace) obtained by adding the two subspectra (F, upper traces). Phases used are $\Phi_1 = y$, $\Phi_2 = (x, -x)$, $\Phi_3 = (8x, 8(-x))$, $\Phi_4 = (x, x, -x, -x, y, y, -y, -y)$, $\Phi_5 = (4x, 4y)$, $\Phi_6 = (-x, -x, x, x, -y, -y, y, y)$, $\Psi_1 = x$, $\Psi_2 = x$ or $-x$ (according to the choice of the subspectra), acquisition phase = $(x, -x, -x, x, y, -y, -y, y, -x, x, x, -x, -y, y, y, -y)$.

Results and Discussion

The delay in the HMBC during which the long-range H-C correlations are established was optimized for a hypothetical coupling constant of 5 Hz. The resulting spectrum showed uniformly intense cross peaks in the region connecting C1 and H2' resonances, whereas the C2'-H1 region showed important differences in intensity for the various cross peaks (data not shown). This observation suggests uniform $^3\text{J}(\text{C1-H2}')$ coupling constants with values close to 5 Hz, but a less uniform distribution for the $^3\text{J}(\text{H1-C2}')$ coupling constants. However, differential relaxation rates as well as any other long-range carbon coupling (Clare et al., 1988) might in part contribute to the latter intensity difference, and the absolute-value character of the cross peaks makes a quantitative evaluation of the coupling constants far from straightforward. Numerous other techniques for measuring ^3J coupling constants have been described in the literature (Poppe and Van

Halbeek, 1991; Uhrin et al., 1992). Poppe et al. (1993) described a ^{13}C -filtered ($^1\text{H}, ^1\text{H}$) ROESY experiment based on the general ^1J -resolved E.COSY approach (Montelione et al., 1989). This experiment resulted in accurate ^3J values for the homogeneous cyclic β -(1-2)-glucan icosamer isolated from *Rhizobium trifolii*. The experiment was performed on a 5 mM natural abundance sample, but the high flexibility of this molecule leads to a completely degenerate ^1H and ^{13}C spectrum, equivalent to that of one single unit (Poppe et al., 1993; Serrano et al., 1993; André et al., 1995a,b). This reduces the information content of the measured coupling constants, as they represent time-averaged values, but it simultaneously enhances the feasibility of the experiment, as the 5 mM sample results in an effective glucose concentration of 100 mM. Despite this high concentration, the resulting experiment took 54 h. A similar experiment on a natural abundance DP13 sample, where no degeneracy exists, would not be feasible, making ^{13}C -labeling essential.

^{13}C -labeling of the molecule was achieved as described above. Mass spectrometry spectra on both the native and ^{13}C -enriched DP13 samples indicated an average mass increase of 37.5 Da, due to the ^{13}C -labeling. Taking into account that the DP13 molecule contains 78 carbon atoms, this gives a mean enrichment of 48%. A similar result close to 50% was found on the basis of integrations made on the non-decoupled ^1H spectrum (Fig. 2A).

The regular HSQC spectrum, where the ^{13}C - ^{13}C coupling constants are not refocused in a constant-time period (Vuister and Bax, 1992), indicates that the labeling is not random. Indeed, we observed a doublet for the C1 resonances (Fig. 2B), but a quintuplet for the C2 correlation peaks (Fig. 2C). ^{13}C enrichment of the C1 position, implying ^{13}C -enrichment of the C2 position, leads to the doublet structure for C1, and the quintuplet structure for the C2 resonances can be explained by the simultaneous presence of $^{13}\text{C}_1$ - $^{13}\text{C}_2$ - $^{12}\text{C}_3$ triplets, leading to a doublet

for C2, and $^{13}\text{C}_1$ - $^{13}\text{C}_2$ - $^{13}\text{C}_3$ triplets on other molecules leading to a triplet structure. Considering the usual bacterial glucose synthesis pathway (Gottschalk, 1986), this implies that the ^{13}C -enriched amino acids have been broken down to the level of a molecule containing two carbons (probably acetyl CoA or acetate), and ^{13}C has been incorporated in a pairwise fashion.

The original experiment as proposed by Poppe et al. (1993) exploits the presence of $^{13}\text{C}_1$ - $^{12}\text{C}_2'$ and $^{12}\text{C}_1$ - $^{13}\text{C}_2'$ carbon pairs at natural abundance. The 50% incorporation of ^{13}C in the present DP13 molecule optimised the number of such carbon pairs, but forced us to introduce an additional step of ^{12}C filtering. The complete sequence is depicted in Fig. 3, and can easily be broken down into three modules: first, a ^{13}C filter is applied in order to select for the t_1 evolution only those protons that are bound to ^{13}C . We used a gradient-enhanced scheme (Fig. 3A) that is quite similar to the solvent suppression scheme

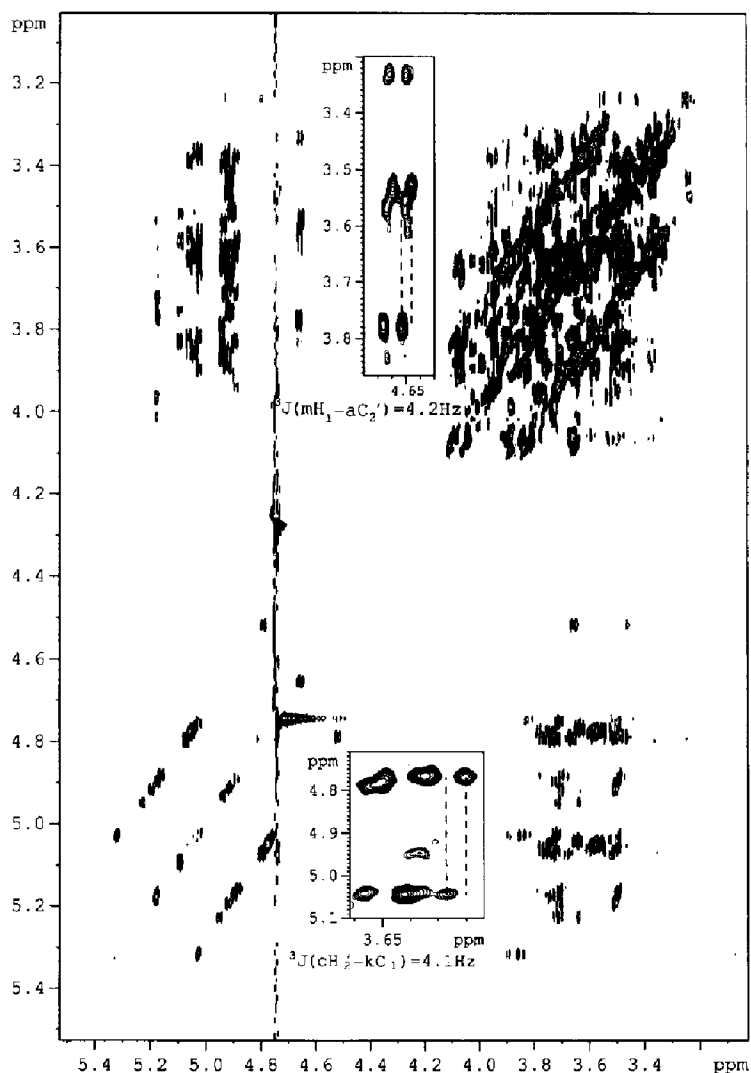


Fig. 4. Final 2D spectrum resulting from adding the two subspectra obtained with the sequence of Fig. 3. The zooms show the aH_2' - mH_1 cross peak and the extraction of the corresponding $^3\text{J}(\text{mH}_1\text{-aC}_2')$ coupling constant (upper), and similarly for the kH_1 - cH_2' cross peak and corresponding $^3\text{J}(\text{kC}_1\text{-cH}_2')$ coupling constant (lower).

TABLE 1
LONG-RANGE ^1H - ^{13}C COUPLING CONSTANTS AND TORSION ANGLES Φ AND Ψ OBTAINED FOR THE CYCLIC GLUCAN OF *BURKHOLDERIA SOLANACEARUM*

Atom pair	$^3J(\text{H1-C2})$ (Hz)	Φ ($^\circ$)	$^3J(\text{C1-H2}')$ (Hz)	Ψ ($^\circ$)
f1-i2	ND	ND	ND	ND
i1-j2	ND	ND	ND	ND
j1-d2	4.1	32	4.0	327
d1-l2	2.2	54	4.2	329
l1-b2	3.0	44	4.7	336
b1-e2	3.4	39	3.8	324
e1-k2	2.9	45	3.9	326
k1-c2	4.1	32	4.1	328
c1-h2	2.9	45	4.1	328
h1-g2	4.0	33	4.2	329
g1-m2	3.0	44	4.3	330
m1-a2	4.2	30	4.0	327

The angles were derived according to a Karplus relationship (Tvaroska et al., 1989) and assuming that the linkages are in the main low-energy zone. The first two values were not determined (ND) due to overlap of the corresponding cross peaks.

used in the ^1H - ^{15}N HSQC experiment (Wider and Wüthrich, 1993). When the first gradient is applied, ^{13}C -bound proton magnetization is in the $I_z S_z$ state, whereas all other magnetization components are in the xy -plane and will be effectively scrambled by G_1 . After refocusing of the proton magnetization, it is stored temporarily along the z -axis, and the second gradient removes effectively all residual terms. The 1D spectrum resulting from this first module is shown in Fig. 3D: no decoupling is applied, and comparison with the regular 1D spectrum clearly shows that all ^{13}C -bound magnetization has disappeared.

In contrast to the ^{13}C half-filter of Poppe et al., our sequence selects no antiphase proton magnetization with respect to the $^1J_{\text{CH}}$ coupling, but pure in-phase proton magnetization (term I_x). This magnetization will evolve during t_1 under the influence of both the chemical shift and the $^1J_{\text{CH}}$ scalar coupling term, and terms of the form $I_x \cos(\omega_1 t_1) \cos(\pi J t_1)$ will enter the NOESY mixing time (Fig. 3B). The length of the mixing time should be a compromise between two requirements: it should be long enough to allow an efficient transfer of proton magnetization between the H1 and H2' positions (Fig. 3E), but it should not be too long such that ^{13}C T_1 relaxation will destroy the E.COSY-type pattern that was constructed during t_1 . Intuitively, the second requirement can be understood as follows: during t_1 , two populations of proton spins can be distinguished, depending on the state of the attached ^{13}C spin. During the NOE mixing time, we want this relationship to be conserved, but it will tend to disappear due to T_1 relaxation. If the mixing time is so long that the correlation between the initial and final ^{13}C spin states has completely disappeared, no displacement in ω_2 representative for the 3J value will be observed (Harbison, 1993). In the case of the cyclic glucan, both requirements can easily be fulfilled by using a short mixing time of 100 ms, as the H1-H2' distances are all very short (Lippens et al., 1996).

After the mixing time, we apply a ^{12}C filter that is similar to the one used for distinguishing NOEs in macromolecular complexes in which one of the components has been enriched with a stable isotope (Otting and Wüthrich, 1989; Fesik et al., 1991; Weber et al., 1991) or for distinguishing intra- from inter-subunit NOE cross peaks in symmetrical homodimers (Lee et al., 1994; Zhang et al., 1994). The same two ^{13}C 90° pulses that are used for ^{12}C selection (once with the phases Ψ_1 and Ψ_2 equal and once with these phases opposite) have to be applied at the end of the filter, in order to maintain the ^{13}C spin state (Fig. 3C). The failure of applying those pulses leads to E.COSY-type cross peaks, which for the two spectra are oppositely shifted in ω_2 with respect to the 3J coupling value, making the addition of the two subspectra in order to produce a ^{12}C -filtered spectrum impossible. The effect of the ^{12}C filter is shown in the 1D trace of Fig. 3F: the diagonal peaks (^{13}C -bound in ω_1 and in ω_2) disappear almost completely, and the only intensity that remains will be found entirely in the cross peaks. In the resulting 2D spectrum (Fig. 4), suppression of the diagonal peaks at the level of the anomeric proton resonances was optimized by introducing a correction factor of 1.08 when adding both subspectra. Some residual diagonal peaks remain for the other proton resonances, due to the imperfect tuning of the ^{12}C filter with respect to the different $^1J_{\text{CH}}$ coupling constants (ranging from 162 to 175 Hz for the anomeric carbons, and from 148 to 150 Hz for the C2 carbons). This imbalance makes a simultaneous cancellation of all diagonal peaks impossible (Otting and Wüthrich, 1990).

The zoomed region in the upper half of Fig. 4 shows an enlargement of the aH2'-mH1 cross peak: in ω_1 , the central frequency of the doublet is that of the aH2' proton, and we observe the doublet with respect to the $^1J_{\text{HC}}$ coupling constant of 145.8 Hz. In ω_2 , both lines correspond to a ^{12}C -bound mH1 proton, but the upper line of the ω_1 doublet is displaced with respect to the lower one by 4.2

Hz, which is the value for the corresponding 3J (mH1-aC2') coupling constant. In the other quadrant of the spectrum, H2 magnetization is observed and the second insert shows a zoom of the kH1-cH2' cross peak. The upper triplet (corresponding to cH2' magnetization coupled through a long-range 3J coupling constant to a k ^{13}C nucleus in a well-defined state) is displaced by 4.1 Hz with respect to the lower one, corresponding to the cH2' proton bound to a k ^{13}C in the other state. In both cases the fine structure of the observed cross peak (a doublet for the anomeric protons, and a triplet for the H2 protons) increases the level of confidence for the measurement of the coupling constant: indeed, we can measure the displacement of every component of the multiplet at $\omega_1 + ^1J/2$ with respect to the corresponding component in the multiplet at $\omega_1 - ^1J/2$. From this multiple measurement, we estimated errors of ± 0.2 Hz on the 3J values reported in Table 1.

In the 2D spectrum of Fig. 4, the presence of intra-residue H5-H1 cross peaks, despite the combined ^{13}C and ^{12}C filters, stems from glucose residues that contain a ^{13}C but a ^{12}C nucleus, and is compatible with the pairwise incorporation of ^{13}C nuclei (vide supra). From these cross peaks, coupling constants for H1-C5 smaller than 0.5 Hz were measured, in agreement with the very weak cross peaks observed in the HMBC.

Using both quadrants, 10 values of both 3J couplings could be extracted (Table 1). The missing values could not be determined because of heavy overlap of the corresponding cross peaks. Finally, it should be noted that the single α -(1-6) linkage can equally be characterized by the same procedure, as we can measure the coupling constants between H6-C1 and H6'-C1 (the notation H6-H6' being at this moment arbitrary). The values found are $^3J(\text{aC1-fH6}) = 2.4$ Hz, and $^3J(\text{aC1-fH6}') = 3.0$ Hz.

Relaxed energy maps for β -sophorose show three predominant zones of low energy, with the main low-energy region at $30^\circ < \Phi < 50^\circ$ and $310^\circ < \Psi < 350^\circ$ (Dowd et al., 1992; André et al., 1995b). A comparison of the calculated energy map with a map showing the H1-H2' interproton distances of β -sophorose in the Ramachandran map (York, 1995), together with the observed strong NOEs for the H1-H2' pairs (Lippens et al., 1996), indicates that all β -(1-2) bonds of the cyclic OPG of *B. solanacearum* are situated in this main low-energy zone. The measured coupling constants can help us to better locate the different glycosidic linkages in the Ramachandran map, and in Table 1 we list the values of both Φ and Ψ assuming that the linkages are in the main low-energy zone. However, caution has to be exercised when interpreting the measured coupling constants in terms of torsional angles. Indeed, the majority of experimental points that were used for the actual parametrization of the Karplus relationship concern a series of conformationally rigid carbohydrate derivatives with dihedral angles be-

tween 90° and 270° (Tvaroska et al., 1989). As the authors had not yet prepared rigid compounds containing fixed C-O-C-H segments having dihedral angles outside this region, they included three experimental values for compounds where the dihedral angles were not directly determined by X-ray crystallography. Therefore, we believe that for our compound, characterized mainly by dihedral angles outside of the (90° , 270°) region, the current parametrization ($^3J_{\text{CH}} = 5.7 \cos^2(\Phi) - 0.6 \cos(\Phi) + 0.5$) and thus the angles derived from the coupling constant values have to be used with caution. We hope that consistency between the NMR-derived distances and dihedral angles determined for the cyclic OPG of *B. solanacearum* will actually help to improve the parametrization.

Conclusions

We have measured a major part of the interglycosidic 3J coupling constants on a partially ^{13}C -enriched sample of the cyclic osmoregulated periplasmic glucan of *B. solanacearum*. These coupling constants, combined with an accurate measurement of interglycosidic distances, are currently being used to derive a detailed atomic model of the cyclic glucan that might shed light on the biological role of these molecules and allow us to establish whether the cavity of these cyclic compounds is compatible with the capability of complexing host molecular signals.

Acknowledgements

We thank Prof. P. Albersheim (Complex Carbohydrate Research Center, University of Georgia) for access to the mass spectrometer and Dr. W.S. York for performing the MALD-TOF MS analysis. Dr. J.-M. Nuzillard (Reims, France) contributed through several fruitful discussions, and we would also like to thank the referees for constructive remarks. The 600 MHz facility used in this study was funded by the Région Nord-Pas de Calais (France), the CNRS and the Institut Pasteur de Lille. Part of this work was performed as a collaborative effort of the Laboratoire Européen Associé 'Analyse structure-fonction des biomolécules' (CNRS, France and FNRS, Belgium).

References

- André, I., Mazeau, K., Taravel, F.R. and Tvaroska, I. (1995a) *Int. J. Biol. Macromol.*, **17**, 189–198.
- André, I., Mazeau, K., Taravel, F.R. and Tvaroska, I. (1995b) *New J. Chem.*, **19**, 331–339.
- Bax, A. and Summers, M.F. (1986) *J. Am. Chem. Soc.*, **108**, 2093–2094.
- Bax, A. and Ikura, M. (1991) *J. Biomol. NMR*, **1**, 99–104.
- Breedveld, M.W. and Miller, K.J. (1994) *Microbiol. Rev.*, **58**, 145–161.
- Clore, G.M., Bax, A., Wingfield, P. and Gronenborn, A.M. (1988) *FEBS Lett.*, **238**, 17–21.
- Dowd, M.K., French, A.D. and Reilly, P.J. (1992) *Carbohydr. Res.*, **233**, 15–34.

- Fesik, S.W., Gampe, R.T., Eaton, H.L., Gemmecker, G., Olejniczak, E.T., Neri, P., Holzman, T.F., Egan, D.A., Edalji, R., Simmer, R., Helfrich, R., Hochlowski, J. and Jackson, M. (1991) *Biochemistry*, **30**, 6574–6583.
- Gottschalk, G. (1986) *Bacterial Metabolism*, Springer, New York, NY, U.S.A.
- Harbison, G.S. (1993) *J. Am. Chem. Soc.*, **115**, 3026–3027.
- Ikura, M., Kay, L.E. and Bax, A. (1990) *Biochemistry*, **29**, 4659–4667.
- Kay, L.E., Ikura, M. and Bax, A. (1991) *J. Magn. Reson.*, **91**, 84–92.
- Lee, W., Harvey, T.S., Yin, Y., Yau, P., Litchfield, D. and Arrowsmith, C.H. (1994) *Nature Struct. Biol.*, **1**, 877–890.
- Lippens, G., Talaga, P., Wieruszkeski, J.-M. and Bohin, J.-P. (1995) In *Spectroscopy of Biological Molecules* (Eds., Mertin, J.C., Turrell, S. and Huvenne, J.-P.), Kluwer, Dordrecht, The Netherlands.
- Lippens, G., Wieruszkeski, J.-M., Talaga, P., Bohin, J.-P. and Desvaux, H., *J. Am. Chem. Soc.*, **118**, 7227–7228.
- Marion, D., Ikura, M., Tschudin, R. and Bax, A. (1989) *J. Magn. Reson.*, **85**, 393–399.
- Montelione, G.T., Winkleer, M.E., Rauenbuehler, P. and Wagner, G. (1989) *J. Magn. Reson.*, **82**, 198–204.
- Otting, G. and Wüthrich, K. (1989) *J. Magn. Reson.*, **85**, 586–594.
- Otting, G. and Wüthrich, K. (1990) *Q. Rev. Biophys.*, **23**, 39–96.
- Poppe, L. and Van Halbeek, H. (1991) *J. Magn. Reson.*, **93**, 214–217.
- Poppe, L., York, W.S. and Van Halbeek, H. (1993) *J. Biomol. NMR*, **3**, 81–89.
- Serrano, G., Franco-Rodriguez, G., Gonzalez-Jimenez, I., Tejero-Mateo, P., Molina Molina, J., Dobado, J.A., Mégias, M. and Romero, M.J. (1993) *J. Mol. Struct.*, **301**, 211–226.
- Talaga, P., Fournet, B. and Bohin, J.-P. (1994) *J. Bacteriol.*, **176**, 6538–6544.
- Talaga, P., Stahl, B., Wieruszkeski, J.-M., Hillenkamp, F., Tsuyumu, S., Lippens, G. and Bohin, J.-P. (1996) *J. Bacteriol.*, **178**, 2263–2271.
- Tvaroska, I., Hricovini, M. and Petrakova, E. (1989) *Carbohydr. Res.*, **189**, 359–362.
- Uhrin, D., Mele, A., Boyd, J., Wormald, M.R. and Dwek, R.A. (1992) *J. Magn. Reson.*, **97**, 411–418.
- Vuister, G. and Bax, A. (1992) *J. Magn. Reson.*, **98**, 428–435.
- Weber, C., Wider, G., Von Freyberg, B., Traber, R., Braun, W., Widmer, H. and Wüthrich, K. (1991) *Biochemistry*, **30**, 6563–6574.
- Wider, G. and Wüthrich, K. (1993) *J. Magn. Reson.*, **B102**, 239–241.
- York, W.S. (1995) *Carbohydr. Res.*, **278**, 205–225.
- Zhang, H., Zhao, D., Revington, M., Lee, W., Jia, X., Arrowsmith, C. and Jardetsky, O. (1994) *J. Mol. Biol.*, **238**, 592–614.